RQC | Russian Quantum Center

AIJR Abstracts

Abstracts of Conference on the Fundamentals of the Physics of Ultracold Atoms and Ions

Editors
Evgeny Anikin
Semyon Zarutskiy
Vasiliy Vinogradov

Organized by
Russian Quantum Center, Russia
19 August 2022

AIJR

2023

Series: AIJR Abstracts

Browse AIJR Abstracts Series at-

https://books.aijr.org/index.php/press/catalog/series/abstracts

Evgeny Anikin
Semyon Zarutskiy
Vasiliy Vinogradov
(Editors)

Abstracts of Conference on the Fundamentals of the Physics of Ultracold Atoms and Ions

19 August 2022

Organized by

RQC Russian Quantum Center

Published by
AIJR Publisher, Dhaurahra, Balrampur, India 271604

Abstracts of Conference on the Fundamentals of the Physics of Ultracold Atoms and Ions
19 August 2022

Editors

Evgeny Anikin
Russian Quantum Center (RQC)
Laboratory of Quantum Computations on Cold Trapped Ions

Semyon Zarutskiy
Russian Quantum Center (RQC)
Laboratory of Quantum Computations on Cold Trapped Ions

Vasiliy Vinogradov
Russian Quantum Center (RQC)
Laboratory of Ultracold Fermions

Conference Organizer
Russian Quantum Center, Russia

Conference Venue
Office of the Russian Quantum Center (Moscow, Bolshoi Boulevard, 30, Building 1, G7)

ISBN: 978-81-961472-1-1
DOI: https://doi.org/10.21467/abstracts.149

Type
Abstract Book
Series
AIJR Abstracts

Published
23 May 2023

Number of Pages
26

Copyeditor
Augustine Gomes

Imprint
AIJR Books

Published by
AIJR Publisher, Dhaurahra, Balrampur, India 271604

Disclaimer

Abstracts of Conference on the Fundamentals of the Physics of Ultracold Atoms and Ions

Russian Quantum Center

Table of Contents

About the Conference

The "Conference on the Fundamentals of the Physics of Ultracold Atoms and Ions" was conducted by the Russian Quantum Center and the State Atomic Energy Corporation Rosatom in parallel with the eponymous summer school. The school was held on July 11–August 19, 2022 on the territory of the RQC.

During the summer school, the participants conducted various research projects in the rapidly developing field of quantum computation with ultracold atoms and trapped atomic ions. In addition, introductory lectures on quantum mechanics, quantum computer science and laser cooling were given in the first two weeks. The research topics included the operations with atomic beams, ion trapping, laser light modulation, quantum algorithms, etc. The results of the projects were presented on the conference.

The Participants, School Lecturers & Project Supervisors of the Summer School

Conference Date: August 19, 2022

Place: Office of the Russian Quantum Center (Moscow, Bolshoi Boulevard, 30, Building 1, G7)

Committees

Conference chairs
Andrey Turlapov Ultracold fermions group leader in the Russian Quantum Center Corresponding member of the Russian Academy of Sciences
Kirill Lakhmanskiy Quantum computing on cold ions group leader in the Russian Quantum Center PhD at the Leopold-Franzens University of Innsbruck (Austria)
Academic secretary
Semyon Zarutskiy Department of Quantum Electronics, Faculty of Physics, Moscow State University RQC Quantum computing on cold ions group
Summer school lecturers & project supervisors
Andrey Turlapov Ultracold fermions group leader in the Russian Quantum Center Corresponding Member of the Russian Academy of Sciences
Kirill Lakhmanskiy Quantum computing on cold ions group leader in the Russian Quantum Center PhD at the Leopold-Franzens University of Innsbruck (Austria)
Georgy Shlyapnikov Scientific Director of the Russian quantum center Professor at the University of Amsterdam
Jacob Biamonte, PhD in physics, Doctor of Science
Artur Matveev, PhD in physics
Olga Lakhmanskaya, PhD in Physics
Evgeny Anikin, PhD in Physics
Vasiliy Vinogradov
Kirill Karpov
Anton Efremov
Ekaterina Efremova
Mikhail Popov
Kirill Khoruzhii
Trofim Ruzaikin
Ilya Mosaki
Lianna Akopyan
Elnury Suleimen

Abstracts of Conference on the Fundamentals of the Physics of Ultracold Atoms and Ions

RQC Russian Quantum Center

Optimization of The Imaging System for Trapped $^{40}Ca^+$ Ions

Zarutskiy S.*, Lakhmanskaya O.

Quantum computing on cold ions group, Russian Quantum Center, Moscow, Russia

*Corresponding author

Keywords: Ion trapping, Paul trap, ion imaging system, 2f- and 4f- lens configuration

1. Introduction

Quantum computers based on trapped ions is one of the most promising platforms for quantum computation. One of the key parts for such a platform is the imaging system. It comprises of a set of lenses including the objective mounted on a vacuum chamber, which collects the photons emitted by the trapped ions and focuses them on the camera matrix. Such system must satisfy the main requirements: efficient collection of the ions radiation to maximize the signal to noise ratio and the ability to distinguish different ions in the chain.

2. Modeling

We examined two systems based on 2f- and 4f- lens configuration. Both of them were modeled in the Zemax package. Despite the fact that the lenses formed a 4f- system intended to reduce spherical aberrations, the beam size calculated in the approximation of geometric optics on the camera matrix had a radius of about 70 μm. This significantly exceeded the Airy disk radius of approximately 3 μm (see Fig. 1).

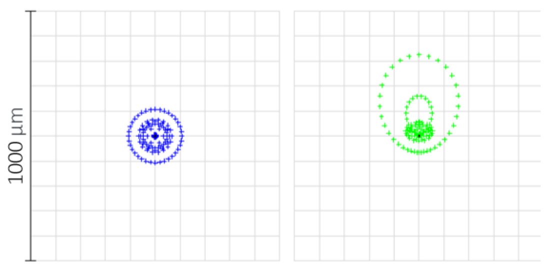

Optical system length 465 mm	Light source in the optical axis	Light source moved radially for 100 μm
Root mean square radius, μm	68	115
Airy dick radius, μm	3	

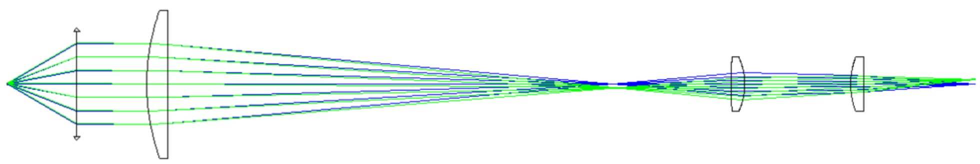

Fig.1: *4f lens configuration*

The second setup consisted of just two lenses: one with a 33 mm effective focal length mounted on a vacuum chamber (NA ≈ 0.5) and another with a 500 mm focal length. According to Zemax simulation, geometric optics approximation gives a spot size on the camera matrix of 1.1 μm, which is smaller than the Airy disk radius of approximately 6 μm (see Fig.2).

DOI: 10.21467/abstracts.149 ISBN: 978-81-961472-1-1 (eBook)

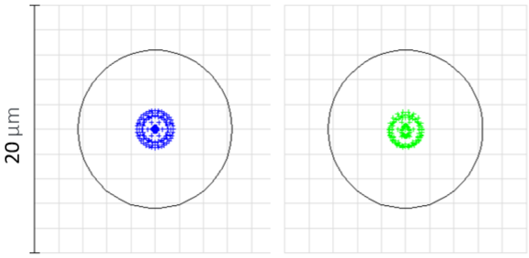

Optical system length 552 mm	Light source in the optical axis	Light source moved radially for 100 µm
Root mean square radius, µm	1.1	1.1
Airy dick radius, µm	6	

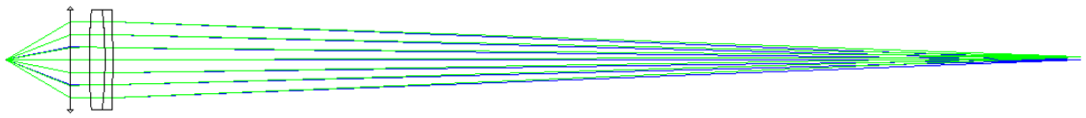

Fig. 2: *2f lens configuration*

3. Results

Based on the simulations we found suitable lenses and installed them in the experimental setup. Finally, the image of the ions in the trap was obtained. On the left in Fig. 3 is a vertical line of cold trapped ions, and on the right is nothing but radiation reflected from the electrodes and background noise.

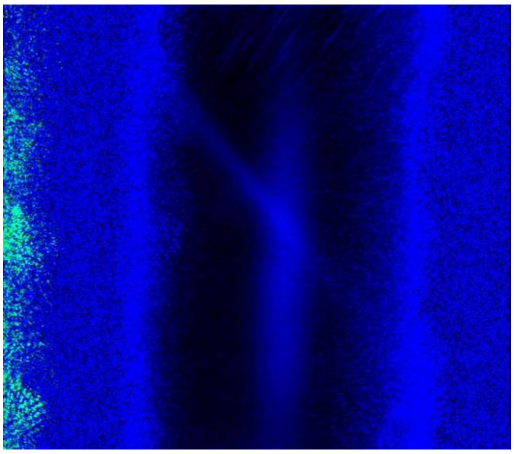

Cloud of ions in the center of the picture

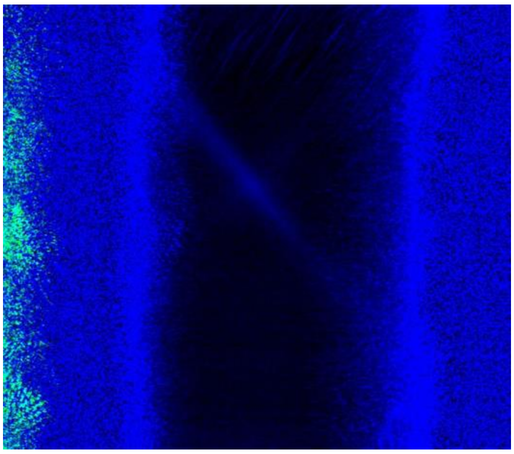

Reflected radiation and background noise

Fig. 3: *Trapped ions cloud*

ISBN: 978-81-961472-1-1

Series: AIJR Abstracts

DOI: 10.21467/abstracts.149

Electrically Induced Transparency in ^{6}Li Atoms

Dyadkin K. D.[1*], Ruzaikin T. D.[2,3], Khoruzhii K. A.[2,3]

[1]National Nuclear Researchers University “MEPhI”, Moscow, Russia
[2]Moscow Institute of Physics and Technology, Dolgoprudny, Moscow Region, Russia
[3]Russian Quantum Center, Moscow, Russia

*Corresponding author

1. Introduction

The effect of electrically induced transparency occurs when a three-level system with one forbidden transition is exposed to strongly coherent radiation. Under certain conditions, the absorption in the medium drastically reduced. As a result, sharp jump in the dispersion of light in the medium near the resonance point appears. This leads to a decrease in the group velocity of light. The effect of electrically induced transparency can find applications in cooling chains of atoms, frequency conversion, and creation of optical quantum memory. In this work, we conducted an experiment to observe the effect of electrically induced transparency using lithium atomic vapor cell.

2. Experiment

The experimental setup is shown in the Fig. 3. The main transition of the Li_6 atoms are the D1 line (see Fig. 1). Transitions between $F = 1/2$ and $F' = 1/2, 3/2$ as well as between $F = 3/2$ and F' levels are allowed whereas transitions between $F = \frac{1}{2}$ and $F = \frac{3}{2}$ are forbidden. The laser used in this work was frequency calibrated. The calibration was carried out by obtaining a saturated spectroscopy in D1 line of Li_6. The two-pass optical scheme involved an acousto-optical modulator to change the frequency of the laser beam. The ^{6}Li atoms are affected by the bichromatic beam which consisted of two beams with orthogonal linear polarizations and different intensities. The main beam is tuned to the transition between $F = 3/2$ and F' with the intensity of 11 mW/cm^2, and the signal beam was set to go from $F = 1/2$ to F' with the intensity of 2 mW/cm^2.

3. Results

In our experiment, we observed the effect of electro-induced light transparency on lithium atoms and investigated the behavior of the effect depending on temperature and relative beam intensities. We obtained the width of the EIT resonance for the D1 line of approximately 1.2 MHz.

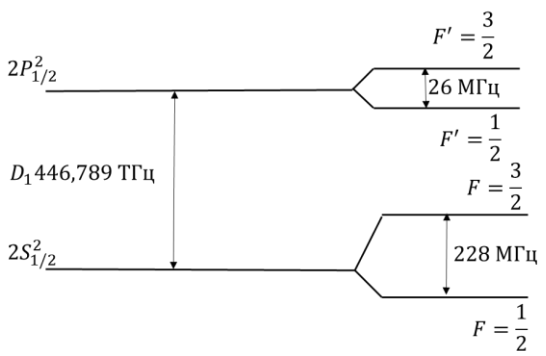

Fig.1: *A schematic energy level diagram for Li_6*

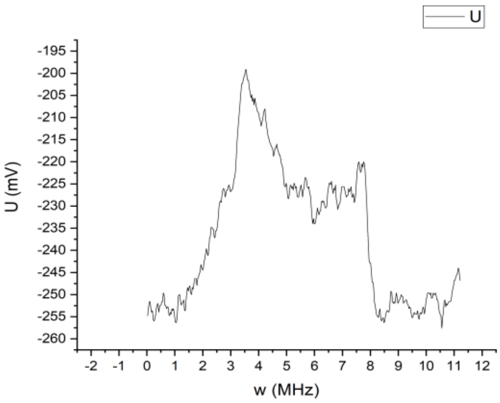

Fig.2: *Dependence of the intensity of the signal beam on the frequency difference*

DOI: 10.21467/abstracts.149 ISBN: 978-81-961472-1-1 (eBook)

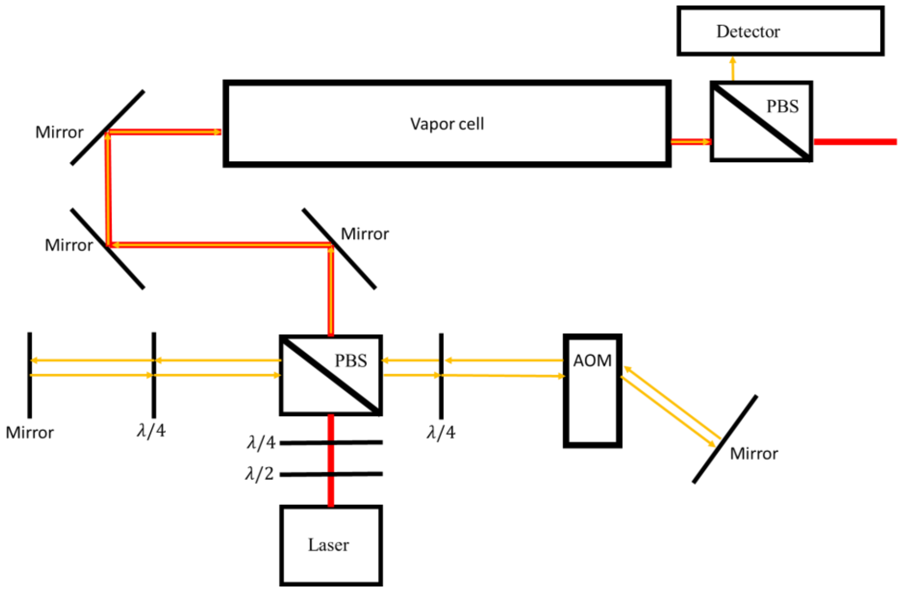

Fig.3: *Experimental setup*

References

1. *J.Fuchs, G.J.Duffy, W. J. Rowlands and A.M. Akulshin*, "Electromagnetically induced transparency in Li", J. Phys. B: At. Mol. Opt. Phys.39(2006) 3479–3489

2. *Scully M.O., Zubairy M.S.* Quantum Optics. – Cambridge: Cambridge University Press, 1997.

ISBN: 978-81-961472-1-1

Series: AIJR Abstracts

DOI: 10.21467/abstracts.149

Measurement of ^{6}Li Atomic Beam Properties

Goloshchapov M. Y.[1*], Khoruzhii K. A.[1,2]

[1]Moscow Institute of Physics and Technology, Dolgoprudny, Moscow Region, Russia
[2]Russian Quantum Center, Moscow, Russia

*Corresponding author
Keywords: ^{6}Li, atomic beam, number of atoms, collimation angle, laser spectroscopy

1. Introduction

Laser cooling is used for frequency standards, quantum simulators, research of ultracold gases and etc. To get large number of ultracold atoms in magneto-optical trap (MOT) atomic beam with small collimation angle and substantial particle flux is required. Optimal parameters of atomic beam are defined by setup of MOT and Zeeman slower and limited by configuration of oven and collimation tube, which are used for melting solid lithium into vapor and focusing it into a beam. Objective of this work was to find optimal temperatures of existing oven and measure atomic beam properties.

2. Experiment

Experimental setup to measure collimation angle and flux is shown on fig.1. Laser beam perpendicular to atomic beam was used to get spectrum of fluorescence of $^{2}S_{1/2} \rightarrow {}^{2}P_{3/2}$ transition. Fitting this spectrum by sum of two Voigt profiles yields Doppler broadening, which was used to calculate perpendicular velocities and subsequently the collimation angle. In order to control that the beams were perpendicular to each other maximums of signals from "moving" atoms and "fixed" atoms in saturated absorption spectroscopy were aligned. Additional laser directed towards atomic beam was used to measure longitudinal speed by means of Doppler shift.

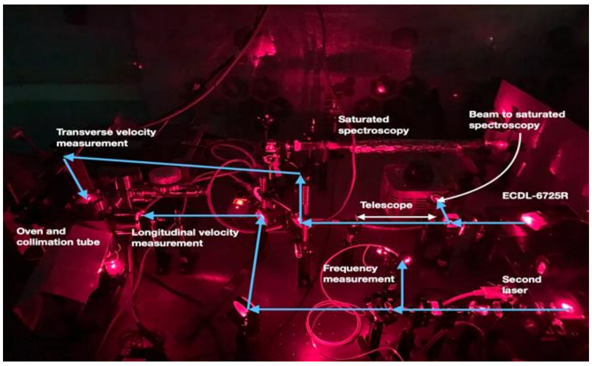

Fig.1: *Experimental setup*

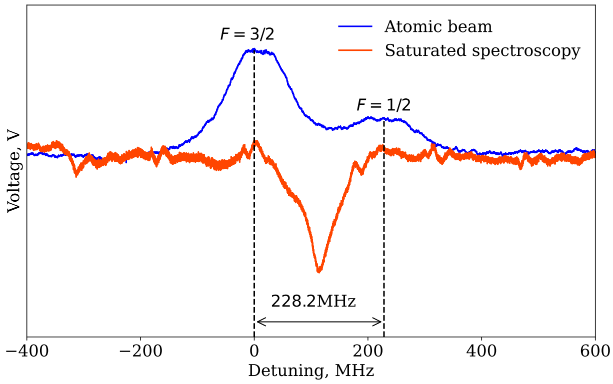

Fig.2: *^{6}Li fluorescense spectrum for $^{2}S_{1/2} \rightarrow {}^{2}P_{3/2}$ transition*

DOI: 10.21467/abstracts.149 ISBN: 978-81-961472-1-1 (eBook)

3. Results

Treating $^2S_{1/2} \rightarrow {}^2P_{3/2}$ transition as Λ-system it was shown that power of spontaneous fluorescence can be approximated by $A\left(1-e^{-\alpha\sqrt{s}}\right)$, which gives A to calculate flux of atomic beam a $N = \frac{3}{4}\frac{A}{\hbar\omega}\frac{4\pi}{\Omega}$, where ω – resonant frequency, Ω – solid angle detected by photomultiplier, s – saturation parameter. Due to its asymptotic nature A can be defined with < 1% error. We can also obtain some information about the system using,

$$\alpha = \frac{C_1 C_2}{\sqrt{2\left(C_1^2+C_2^2\right)}}\frac{\Gamma}{\sigma}\sqrt{\frac{t}{\tau}}$$

where C_1, C_2 – coupling coefficients, σ – Doppler broadening, Γ – natural linewidth, t – time of interaction with laser, τ – excited state lifetime.

Temperatures of oven that yield theoretically optimal collimation angle were found. Number of atoms per second was calculated in two ways: integrating the spectrum and using the asymptotic formula. Asymptotic approach showed to be more precise for counting flux of atomic beam.

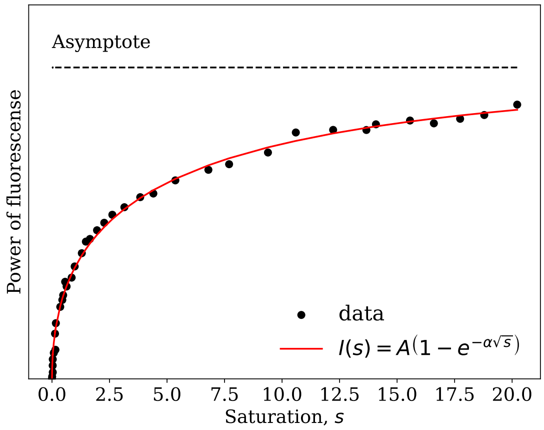

Fig.3: *Power of fluorescence*

The spectra of fluorescence were approximated by sum of two Voigt profiles to calculate collimation angle via Doppler broadening of atomic beam. Doppler shift was measured to calculate the longitudinal velocity.

ISBN: 978-81-961472-1-1

Series: AIJR Abstracts

DOI: 10.21467/abstracts.149

Phonon Modes χ3 Non-linearity in Ion Chains

Gorshenin V. L[1*]., Anikin E. V.[2]

[1]Moscow Institute of Physics and Technology, Dolgoprudny, Moscow Region, Russia
[2]Russian Quantum Center, Moscow, Russia

*Corresponding author
Keywords: Coulomb crystal, anharmonic oscillation, Kerr-type coupling

Trapped ions are one of the most promising systems suitable for quantum computation. In Coulomb crystals consisting of trapped ions, high-fidelity single-qubit and entangling gates have been demonstrated, and quantum simulations of long-range Ising spin chains have been performed. To generate couplings and create entanglement between different ions, collective vibrational excitations (phonon modes) of the Coulomb crystal are utilized. Due to intrinsic nonlinearity of the Coulomb interaction, there are various types of nonlinear interactions between the phonon modes. They are one of the sources of the gate's infidelity in the ion chain, and they can also be used to perform quantum nondemolition measurements.

In this work, we study the Kerr-type nonlinearities of the phonon modes of the linear Coulomb crystal. The interaction part of the phonon modes Hamiltonian with account for the Kerr and cross-Kerr terms reads $H = \sum_{\alpha,\beta,\gamma} c^{(1)}_{\alpha,\beta,\gamma} \grave{a}^\dagger_\alpha \grave{a}^\dagger_\beta \grave{a}^\dagger_\gamma + \sum_{\alpha,\beta,\gamma} \hbar\omega^{(2)}_{\alpha,\beta,\gamma} \grave{a}^\dagger_\alpha \grave{a}^\dagger_\beta \grave{a}_\gamma + \sum_{\alpha,\beta,\gamma} c^{(3)}_{\alpha,\beta,\gamma} \grave{a}^\dagger_\alpha \grave{a}_\beta \grave{a}_\gamma + \sum_{\alpha,\beta,\gamma} c^{(4)}_{\alpha,\beta,\gamma} \grave{a}_\alpha \grave{a}_\beta \grave{a}_\gamma + \sum_{\alpha,\beta} c^{(5)}_{\alpha,\beta} \grave{a}^\dagger_\alpha \grave{a}_\alpha \grave{a}^\dagger_\beta \grave{a}_\beta$, where: $\grave{a}^\dagger_\alpha, \grave{a}_\alpha$ are the creation and annihilation operators of the normal mode α , and $c^{(i)}_{\alpha,\beta,\gamma}$- are constants. To find these coefficients for the Coulomb crystal consisting of N ions, we considered the crystal Hamiltonian

$$H = \sum_{j=1}^{j=N} \left(\frac{p^2_{x,j} + p^2_{y,j} + p^2_{z,j}}{2m} + \frac{m\left(\omega^2_{rad} x^2_j + \omega^2_{rad} y^2_j + \omega^2_{ax} z^2_j\right)}{2} \right) + \frac{e^2}{8\pi\epsilon_0} \sum_{j,m=1}^{j,m=N} \frac{1}{\sqrt{\left(x_j - x_m\right)^2 + \left(y_j - y_m\right)^2 + \left(z_j - z_m\right)^2}}$$

where x_j, y_j, z_z are the positios of the ion j, $p_{x,j}, p_{y,j}, p_{z,j}$ are the momenta of the ion j along the axes X, Y, Z, m is the mass of the ion; $\omega_{rad}, \omega_{ax}$ are the radial and axial frequencies of the confining potential. We developed a numerical algorithm to calculate the ions equilibrium positions and found the normal modes spectrum. Then, we expanded the Coulomb potential in Taylor series up to the fourth order in the deviations from the equilibrium positions and expressed the expansion terms through the phonon creation/annihilation operators. For the fourth order, the Kerr and cross-Kerr terms which not change the number of quanta cause the most considerable effect.

DOI: 10.21467/abstracts.149 ISBN: 978-81-961472-1-1 (eBook)

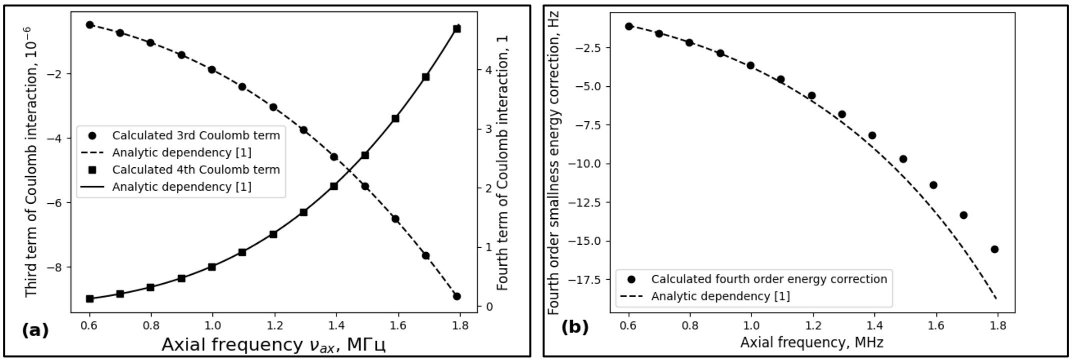

Fig.1: (a) *Coulomb interaction coefficients for axial modes calculated and analytic solution for 2 ion chain and.* **(b)** *Frequency shift correspond fourth order energy correction. Assumed radial frequency is 4 MHz and* $^{40}_{20}Ca^{+}$ *ion.*

Using the obtained coefficients of the nonlinear interactions, we found the corrections to the energies of the phonons Fock states. Also, we compared the third and the fourth orders of the numerically obtained Hamiltonian expansion Coulomb terms the with analytic solution for the two-ion chain [1] presented in Fig.1. For the energy corrections of the fourth order, the comparison with the analytic solution for the two-ion chain [1] are presented in Fig.2. In both cases, there is satisfactory coincidence between the analytical and numerical results. Also, we found the scaling law of the Kerr coupling in the Coulomb crystal.

References

1. X. Rebecca Nie et al., Physics Letters A 373. 4 (2009), c. 422-425

ISBN: 978-81-961472-1-1

Series: AIJR Abstracts

DOI: 10.21467/abstracts.149

Optical Pumping of Lithium 6 Atomic Beam

Shlykov P. Y.[1*], Khoruzhii K. A.[2]

[1]Moscow Institute of Physics and Technology, Dolgoprudny, Moscow Region, Russia
[2]Russian Quantum Center, Moscow, Russia

*Corresponding author
Keywords: ^{6}Li, atomic beam, optical pumping, laser spectroscopy

1. Introduction

Optical pumping plays the main role in slowing atoms in Zeeman slower, which provides the opportunity of interacting with atoms for longer time because of energy level shift. For better deceleration it is essential to change the state of atoms in the beam to the state with the greatest projection of total atomic angular momentum, that is where pumping plays a great role. This will allow to increase the number of trapped atoms in future experiments.

2. Experiment

For this reason, the experiment was conducted to observe the dependence of populations of energy levels on frequency and intensity of pumping laser beam (Fig.1).

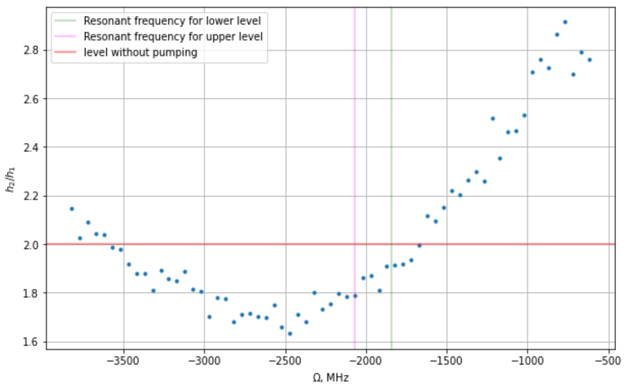

Fig.1: *Pump dependency on frequency*

Atoms were vaporized in the oven and collimated into the narrow beam (Fig.2). The experiment was carried out with the use of two lasers. One of which was pumping atoms in a beam with stable wavelength and intensity, second one was used for scanning state of the beam by various frequencies. The pumping laser was directed towards the propagation of atoms and covered the whole atomic beam, from its parameters the main dependencies were measured. The second laser was directed perpendicular to the line of atomic beam. Small variety for speed of atoms in the beam gave less Doppler shift for frequency. This provided better possibility for collecting data over the distribution of atoms. This was observed by the power of fluorescence of the $^2S_{1/2} \rightarrow {}^2P_{3/2}$ transition. Part of second laser intensity was used for frequency stabilization with saturated spectroscopy. Also, numerical modeling of the pumping process was performed.

Fig.2: *Experimental setup*

DOI: 10.21467/abstracts.149 ISBN: 978-81-961472-1-1 (eBook)

3. Results

Collected data showed main dependencies of effectiveness of pumping on laser frequency in the interval close to resonance wavelength of $^2S_{1/2} \rightarrow {}^2P_{3/2}$ transition and dependency on intensity showed plateau entry. Numerical modeling showed approximate time for the system to enter the steady state and approximate number of atoms, which are being pumped at fixed laser frequencies. Also, it showed dynamic change of the system in the process.

ISBN: 978-81-961472-1-1

Series: AIJR Abstracts

DOI: 10.21467/abstracts.149

Electro-optical Modulator - 2 Harmonics

Chadov I. A.[1,2]

[1]Bauman Moscow State Technical University, Moscow, Russia
[2]Russian Quantum Center, Moscow, Russia

Keywords: Phase modulation, electro-optic modulator.

1. Introduction

This work demonstrates the generation of frequency components of the laser beam modulated by an electro-optic modulator (EOM) with the frequency of 230.5 MHz. This method of laser harmonic generation can be used in experiments with ultra-cold atoms, to excite several transitions simultaneously in ^{6}Li atoms, and in quantum calculations with cold trapped ions. Objective of this work was to generate frequency harmonics using an electro-optical modulator in a monochromatic laser beam and measuring the harmonics power as a function of the amplitude of the signal applied to the electro-optical modulator.

2. Experiment

Experimental setup is shown on fig.1. The laser radiation of horizontal polarization is directed through an optical fiber into the EOM and is focused on the interferometer using a lens. For the most efficient operation, it is necessary that the Gaussian beam fully enters the EOM along the normal. Sinusoidal signal with a frequency of 230.5 MHz and regulated voltage of 0-4.5 V is fed to the EOM, depending on which the level of harmonics of the laser radiation at the output of the EOM changes. The signal applied to the EOM has the form: $U = U_m \sin{(2\pi f_m)}$.

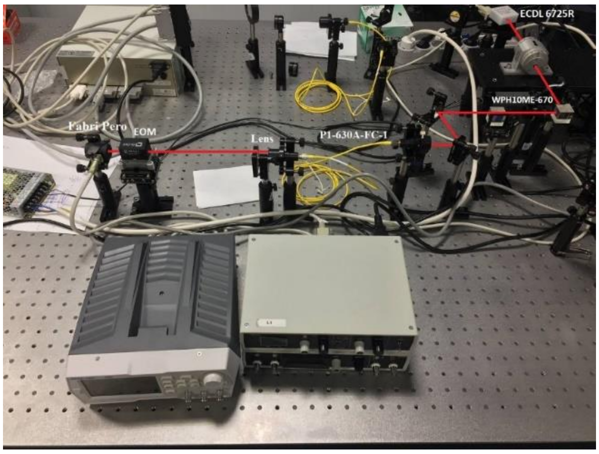

Fig. 1: *Experimental setup*

3. Results

Considering the phase-modulated laser signal at the EOM output, its representation in the form $E(t) = E_0 \sum_{n=-\infty}^{\infty} J_n(\varphi_0) \cos{[(2\pi f_0 + n2\pi f_m)t]}$ was obtained where J_n is the Bessel function, E_0 is the laser amplitude, f_0 is the laser frequency, f_m is the frequency of the sinusoidal signal fed to the EOM, φ_0 is the

DOI: 10.21467/abstracts.149 ISBN: 978-81-961472-1-1 (eBook)

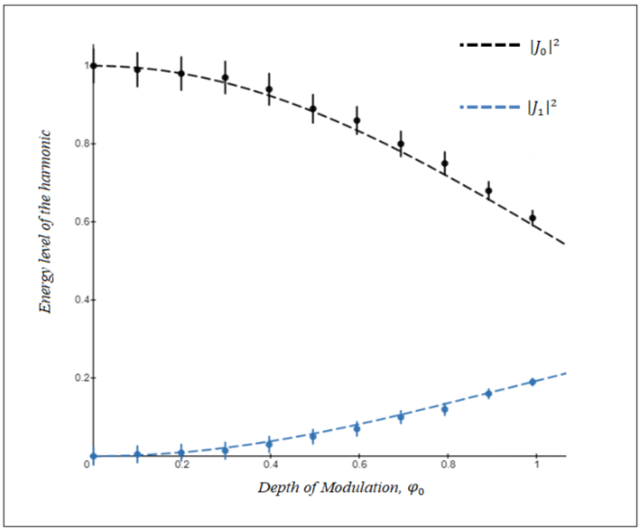

Fig.2: *Plot of the level of the first and second harmonic of the laser as a function of the modulation depth*

modulation depth, which is defined as $\varphi_0 = 0.22 \cdot U_m$. Due to this representation, we can obtain the ratio for the power levels of the first and second harmonics defined as $\frac{|J_0|^2}{|J_1|^2}$.

The harmonic power level was normalized to the laser energy $|E_0|^2$.

ISBN: 978-81-961472-1-1

Series: AIJR Abstracts

DOI: 10.21467/abstracts.149

Light Control via Spatial Light Modulator

Ilia Yukhnovets

Russian Quantum Center, Moscow, Russia

Keywords: spatial light modulator, Gerchberg-Saxton algorithm, holograms, amplitude modulation.

Spatial light modulators are a valuable tool for controlling the properties of the optical field. They have a wide range of applications including optical microscopy, holography, etc. In addition, they can be used for the creation of the optical dipole traps with the ability to quickly change the field properties. The purpose of the current work is to develop and experimentally test a Matlab toolboox for the SLM Hamamatsu X13138 for the future development of the SLM-based optical dipole trap.

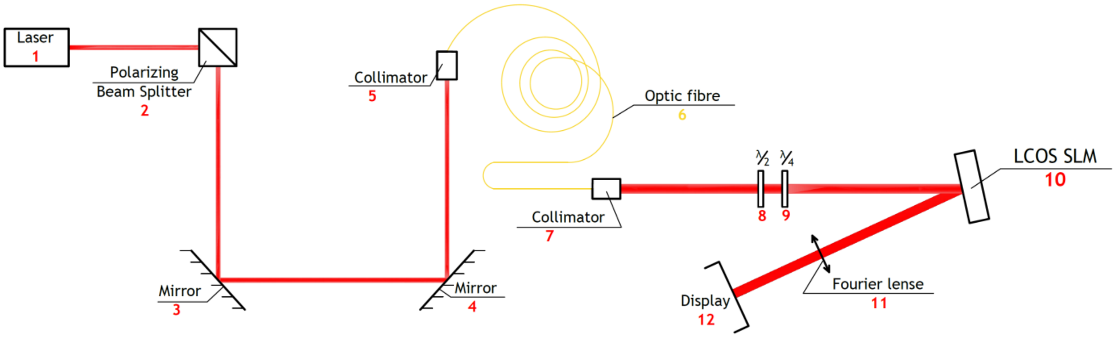

Fig.1: *Experimental setup*

SLM affects the incident beam as a matrix of discrete pixels where each pixel changes the phase and the amplitude of the incident beam. The SLM considered in this work changes only the phase, and its action can be described as

$$A(r) = A_0(r) \cdot e^{i\varphi(r)}, \tag{1}$$

where $A_0(r)$ is a complex amplitude of the input beam, and $\varphi(r)$ is an SLM's phase shift. The field distribution in the Fraunhofer zone is determined by the free field propagation.

The developed toolbox allows to create the wavefronts of various shapes in the Fraunhofer zone using SLM. In particular, it provides the wavefronts similar to those of the standard optical elements such as echelette, axicon and cylindrical lens. Also, more complicated shapes can be created, for example, logotypes and small text fragments. To obtain these wavefronts, the SLM phase shifts are represented as an 1272×1024 array (same as the resolution of the SLM) which is converted to a BMP image and then loaded to the SLM with special software. The values of the phase shifts are calculated either analytically or using Gerchberg-Saxton iterative algorithm.

The author assembled an experimental setup (see Fig. 1) that allows to observe the intensity distribution in the Fraunhofer zone on a screen (12), located in the focal plane of Fourier lens (11). To evaluate the performance of the toolbox, the author compared the images obtained with SLM with the images obtained with the simulated optical elements. The more complicated field distributions were also created. The reached results demonstrated the ability of the developed toolbox to obtain a high degree of control of the optical field in the Fraunhofer zone. Also, it allows to create the ring-shaped beam required for a dipole trap for capturing neutral atoms.

 Published by AIJR Publisher in "Abstracts of Conference on the Fundamentals of the Physics of Ultracold Atoms and Ions", 19 August 2022. Organized by Russian Quantum Center, Russia.
DOI: 10.21467/abstracts.149 ISBN: 978-81-961472-1-1 (eBook)

Diffraction Grating Wavelength Meter using a High-resolution Webcam with Sub-gigahertz Sensitivity

Silaev V. D.

Moscow Institute of Physics and Technology, Dolgoprudny, Moscow Region, Russia

Keywords: wavelength meter, gaussian beam, diffraction grating

1. Introduction

Nowadays tunable lasers are widely used in various fields of science, for example, in laser cooling of atoms. Laser cooling is a technique based on the fact that particles change their momentum after re-emitting photons which they have absorbed due to laser irradiation. In aforementioned technique it is crucial to use a beam tuned to a specific atomic transition. Also, analyzing atomic spectra requires the ability to measure a number of optical signals with close frequencies simultaneously, for instance, D1 and D2 transitions in ^{6}Li atoms have frequencies differing by 10 GHz while having wavelength around 670 nm (relative difference $\sim 2 \cdot 10^{-5}$). Objective of this work is to construct a wavelength meter having properties mentioned above.

2. Experimental setup

Principle of operation of the device is based on diffraction grating properties which allow for spatially splitting beams with different frequencies. Acquired spectrum of a gaussian-mode beam is registered by a high-resolution webcam with pixel size 3.45 × 3.45 μm. Scheme of the constructed device is shown on fig. 1. To compensate the sensitivity to environmental conditions in the laboratory, such as temperature and humidity, and mechanical disturbances, we calibrated the device before every series of experiments. Calibration of the constructed wavelength meter is carried out by using another commercial wavemeter with higher accuracy and a single-mode tunable laser, alternatively, setup can be calibrated with reference to known atomic transitions frequencies.

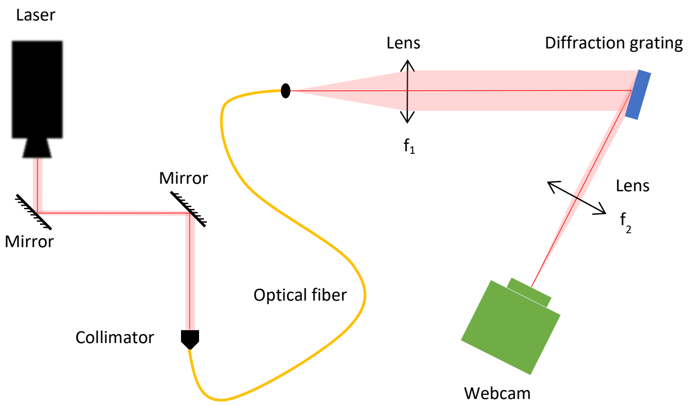

Fig. 1: *Schematic representation of the device*

3. Results

After several series of experiments with wavelengths near 670 nm measured frequency resolution of acquired wavemeter turned out to be 0.6 GHz per pixel while maximum measurement error is equal to 1.5 GHz. Constructed wavelength meter has shown the ability to distinguish frequencies differing by 9 GHz while measured simultaneously and the ability to determine whether laser is in multiple frequency mode.

DOI: 10.21467/abstracts.149 ISBN: 978-81-961472-1-1 (eBook)

Abstracts of Conference on the Fundamentals of the Physics of Ultracold Atoms and Ions

RQC | Russian Quantum Center

RQC | Russian Quantum Center

AIJR Abstracts

Abstracts of Conference on the **Fundamentals of the Physics of Ultracold Atoms and Ions**

Editors
Evgeny Anikin
Semyon Zarutskiy
Vasiliy Vinogradov

Organized by
Russian Quantum Center, Russia
19 August 2022

ISBN 978-81-961472-1-1
9 788196 147211